Pergamon

0301-9322(94)00046-8

Int. J. Multiphase Flow Vol. 20, No. 6, pp. 1071–1083, 1994

0301-9322/94 $7.00 + 0.00

THE SPLIT OF VERTICAL ANNULAR FLOW AT A LARGE DIAMETER T JUNCTION

B. J. AZZOPARDI

Department of Chemical Engineering, University of Nottingham, University Park, Nottingham NG7 2RD, England

(Received 26 December 1993; in revised form 2 May 1994)

Abstract—Measurements and observations have been made of the split of gas–liquid flow at a T junction where the main pipe was vertical and the side arm horizontal. All three pipes connecting to the junction were of 0.125 m dia. The gas and liquid flow rates were chosen to ensure annular flow in the inlet pipe. The resulting data have been compared with existing models.

Key Words: junctions, flow split, data, gas–liquid

1. INTRODUCTION

Junctions are an often necessary feature of many pipelines or pipework systems. For single-phase flows, there are equations which, though empirical, enable engineers to carry out designs. In the case of two-phase flow, however, the number of variables is much larger; in addition there are complicating factors in the partition and mixing of the phases.

The division of two-phase flow at junctions can constitute a major problem when it occurs in a chemical process, power generation or oil and gas production and refinery plant because either phase could pass preferentially into the minor branch of the junction. This maldistribution can have a significant effect on the behaviour of equipment downstream of the junction far exceeding the size of the junction relative to the complete plant. For example, the maldistribution occurring during flow splits at junctions is important when steam injection is being used to effect enhanced recovery of viscous oils, the steam is usually generated at a central point and distributed to a number of wells. This can involve several junctions. In this process it is important to know where the water (either that coming from the boiler because of incomplete evaporation or that due to condensation of steam along the transmission lines) goes to, as water having lost its latent heat is much less effective at lowering the viscosity of the oil.

In the process industries there are many dividing junctions. For example, the pipework feeding a bank of air-cooled heat exchangers or other exchangers mounted in parallel. If these units are operating as condensers with a two-phase feed, maldistribution of the phases will have a direct effect on the heat exchanger performance; those receiving mainly liquid will underperform significantly because the intube heat transfer coefficients during subcooling will be much lower than the corresponding condensation coefficient. Those exchangers receiving mainly vapour will perform slightly better than expected. However, this would not normally be sufficient to compensate for poor performers and the entire bank could operate below specification.

2. PREVIOUS WORK

Table 1 lists sources of data for flow split at T junctions where the main tube was vertical. The experiments were all carried out with low pressure air/water. Figure 1 shows that in most cases the inlet conditions correspond to annular or churn flow with some odd points in other flow patterns. In the figure, the flow pattern boundaries were calculated using the equations suggested by Taitel *et al.* (1980) (bubble/slug; bubble/dispersed bubble and dispersed bubble/churn) and Brauner & Barnea (slug/churn). For the annular/churn transition the equation of McQuillan & Whalley (1985) was used for smaller diameters whilst that of Taitel *et al.* was used in cases with diameters (defined as $D^* = d(\rho_L g/\sigma)1/2$) greater than 9.61.

Table 1. Summary of published data for flow split at a T junction when the main pipe is vertical

Source	Diameter (m)	Diameter ratio	Pressure (bar)	Mass flux (kg/m²s)	Quality (—)	Take-off
Fouda (1975)	0.025	0.75	1.5–3.3	160–660	4.3×10^{-4}–0.39	0.06–0.93
Azzopardi & Baker (1981)	0.032	0.4	1.5	87–111	0.09–0.29	0.0–0.92
Honan & Lahey (1981)	0.038	1.0	1.5	1350–2700	0.001–0.01	0.3–0.7
Azzopardi & Whalley (1982)	0.032	0.4	1.5	83–178	0.35–0.81	0.0–0.25
Zetzmann (1982)	0.024, 0.05, 0.1	0.5, 1.0	2	500–3000	0.005–0.035	0.1–0.8
Azzopardi (1984)	0.032	0.2, 0.6, 0.8, 1.0	1.5	83–178	0.35–0.81	0.0–0.57
Azzopardi (1988)	0.032	1.0	1.5	98–178	0.02–0.86	0.0–1.0
Hewitt *et al.* (1990)	0.032	0.6, 1.0	3	800–2400	0.0033–0.05	0.0–1.0

Annular flow approaching a junction with a vertical main tube and a horizontal side arm have been studied by Azzopardi & Whalley (1982) and Azzopardi (1984, 1988, 1989). They observed that initially the fraction of liquid taken off was greater than the gas fraction but that this was reversed at higher take off. The fraction of liquid taken off decreased with increasing inlet gas and liquid flow rates. At relatively high values of gas take off, the amount of liquid extracted suddenly increased for a small increase in gas take off. An exception to the above behaviour occurred at low liquid inlet conditions when liquid was preferentially extracted. Azzopardi (1989) postulated a model which involved up to three phenomena to explain the trends in the data. The first of these phenomena uses the fact that the momentum of the film is similar to that of the gas and both are much less than that of the drops, assumed to be travelling at the gas velocity. It also relies on the observation (from single phase flow) that the extracted fluid comes from a segment nearest to the side-arm. For annular flow, gas and liquid film from the local segment are assumed to be taken off. They are related by

$$G' = \frac{1}{2\pi}\left[\frac{2\pi L'}{(1-E)K} - \sin\left(\frac{2\pi L'}{(1-E)K}\right)\right] \quad [1]$$

where G' and L' are the fractions of gas and liquid taken off,

$$K = 1.2\left(\frac{d_3}{d_1}\right)^{0.4}$$

E is the fraction of liquid resulting from film stop and L_{seg} is the fraction of liquid entrained, d is the pipe diameter and subscripts 1 and 3 refer to the inlet and side-arm respectively. K is an empirical diameter ratio correction factor suggested by Azzopardi (1984). At higher take-off, Azzopardi (1988) suggested that the gas velocity in the main tube above the junction can fall below

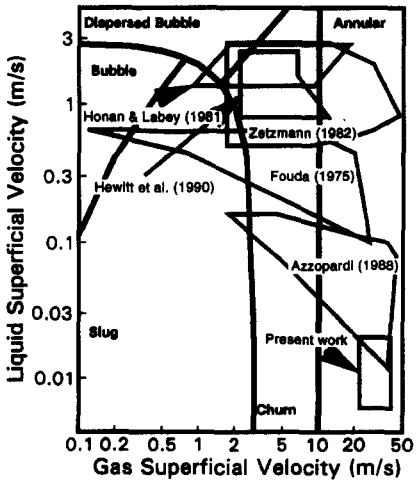

Figure 1. Flow pattern map showing existing flow split data taken from T junctions with vertical main tube (heavy lines indicate flow pattern boundaries, lighter lines denote condition at which data taken).

the flooding velocity and liquid which has passed the junction then falls back and is taken off. The equation of Wallis (1961) was used to determine the conditions at which the liquid starts to fall back, the amount of liquid fall back and the condition at which no liquid is carried up. The third phenomenon is important if the film has a low momentum when it can react to the pressure increase across the junction and slow down. Azzopardi (1989) analysed this process by assuming that the liquid occupies a very small portion of the pipe cross section. The pressure increase along the main pipe is given by

$$P_1 + \frac{\rho_G u_{G1}^2}{2} = p_2 + \frac{\rho_G u_{G2}^2}{2} + k_{12}\frac{\rho_G u_{G1}^2}{2} \quad [2]$$

where p is the pressure and u can be taken as the superficial velocity. The pressure loss coefficient, k_{12}, was calculated from the correlation of Gardel (1957). A similar equation can be written for the liquid film

$$p_1 + \frac{\rho_L u_{f1}^2}{2} = \rho_2 + \frac{\rho_L u_{f2}^2}{2} + D. \quad [3]$$

Here the subscript f refers to the film and D is the energy loss.

Combination of equations indicated that the film velocity can decrease across the junction. In the extreme, the velocity downstream falls to zero. The (critical) gas take off at which this occurs is given by

$$G_c' = 0.715 - \sqrt{0.493 - 0.633\frac{\rho_L u_{f1}^2}{\rho_G u_{G1}^2} + \frac{1.266\,D}{\rho_G u_{G1}^2}}. \quad [4]$$

Azzopardi (1989) argued that D could be taken as 0 as this would be a conservative case. Once the film is stopped, the proportions of this liquid which is extracted from the side-arm can be calculated from the assumption that the liquid emerging is proportional to the shear imposed in the downstream and side arm directions. This yields

$$L_s' = (1 - L_{seg}' - E)\left(\frac{G'^2}{1 - 2G' + G'^2}\right). \quad [5]$$

L_s' is the fraction of liquid resulting from film stop and L_{seg}' is the fraction taken off directly and calculated from [1]. The total liquid taken off is given by the amounts indicated by [1] and [4] (if appropriate) as well as that liquid which falls back because of flooding.

Shoham *et al.* (1987, 1989) developed a model in which the phase maldistribution was the result of centrifugal separation produced by the fluids following a circular path into the side-arm. This model gives reasonable predictions of data. Hwang *et al.* (1988) and Hwang (1986) modelled the phase separation by assuming that there is a zone of influence for each of the two phases from which the fluid is taken off. This is bounded by the channel wall and an appropriate dividing streamline, the position of which are determined from a balance between the dominant forces acting on each phase. Sliwicki & Mikieliwicz (1988) analyse the diversion of the liquid film by considering the local forces at the front corner of the junction. They also calculate the fraction of drops diverted into the side arm. Constants in their equations have been optimised using the data of Azzopardi & Whalley (1982). Lately, Hart *et al.* (1991) have developed a model for gas flow with small liquid content. This was based on Bernoulli equations for each phase along the main pipe and from the main pipe to the side arm. They assume no interaction between the phases. Loss coefficients are described by single phase correlations. Manipulation of the equations results in a relationship between the fraction of liquid taken off through the side arm and the fraction of gas taken off.

This paper describes experiments in which observations and measurements have been made of the split of annular flow at a vertical T junction with 0.125 m dia pipes, i.e. several times the diameter used in previous work.

3. EXPERIMENTAL ARRANGEMENT

3.1. Flow facility

The apparatus used in the experiments is shown schematically in figure 2. Air was drawn from the laboratory by a centrifugal blower through an intake section which contained an orifice plate

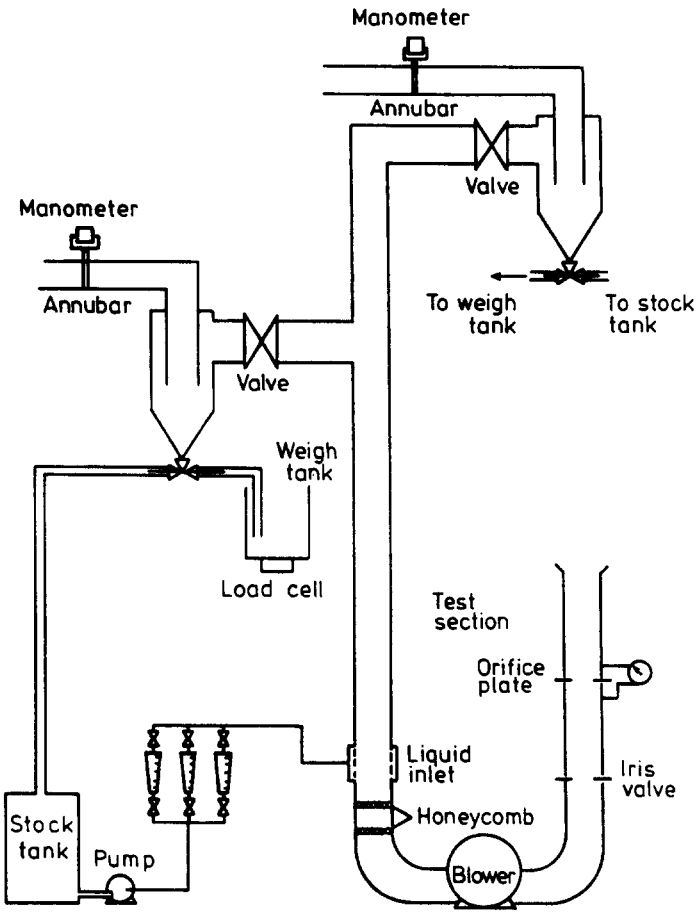

Figure 2. Experimental facility.

to meter the flow rate and an iris valve to regulate the flow. The air was delivered to the bottom of the vertical main tube which was made up of sections of acrylic resin tube of 0.125 m i.d. The water, which was drawn from the stock tank by a centrifugal pump, was metered by one of a group of calibrated variable area flowmeters and introduced into the vertical tube through a porous wall section placed 0.6 m from the bottom. The air entrance section contained a number of layers of aluminium honeycomb to minimize the effects of the bends through which the air entered the vertical test section. The T junction (described in section 3.2. below) was placed 3.0 m from the liquid entry point. In the first series (A) of experiments, this was followed by a further 1.75 m of 0.125 m tube a bend and a horizontal tube which contained a butterfly valve and led to a cyclone. For the second series (B), a further 2 m of 0.125 m dia tube was provided. A 180° bend then brought the flow back down to the original horizontal tube. The side-arm consisted of 0.5 m of 0.125 m tube followed by a butterfly valve. This was connected to a second cyclone. In the series (A) tests, the air flows emerging from the two cyclones were metered using Anubars (multihole pitot-static devices). These were replaced by venturis for the series (B) tests. The water flows were determined from weighing a timed efflux, the flow from either cyclone would be diverted into a weigh tank which was placed on a calibrated load cell. The other water stream was returned to the main stock tank.

3.2. T junction

The T junction used in the present study was machined from an acrylic resin block. The main bore and the side-arm were both 0.125 m dia. To minimize refraction problems when taking still or cine photographs, the outside of the was machined to a square cross section (0.2 × 0.2 m). All surfaces were polished to improve observation. The junction block had flanges at the three ends to mate with the rest of the test section pipework. The inside of the T junction was carefully

machined with sharp corners so as to eliminate the radius of curvature as a possible variable in the experiments.

3.3. *Calibration of equipment*

The liquid emerging from the cyclones diverted into a weigh tank and the amount accumulated over a measured time was recorded. The weigh tank was mounted on a load cell whose output was checked against standard weights. The water inlet rotameters were calibrated by weighing a timed efflux.

The orifice plate for inlet air flow measurement and the Anubars and venturis which measured the outlet air flow rates were all calibrated *in situ* by means of a calibrated turbine meter.

A further check on the instrumentation was provided by the mass balances carried out during the experimental programme. This showed that the sum of the outlet air flow rates were within 10% of that at inlet. Similarly the incoming and exiting water flows showed excellent agreement.

4. RESULTS AND DISCUSSION

4.1. *Observations*

Observations of the flow were possible as both the T junction and the pipes leading to and from it were made of transparent acrylic resin. Direct observations were complemented by high speed video (1000 fps). From these it was seen that at low take-off the liquid film adjacent to the side arm appeared to be diverted into the side-arm. However, a pool of liquid accumulated along the bottom of the side arm pipe at low take-off as the valve in its 'almost closed' position acted as a weir. Under these conditions the gas flow in the side-arm was insufficient to lift the liquid over this weir. The pool of liquid could have forced liquid back into the main pipe where it would have been atomized and carried into the pipe beyond the junction.

At higher take-off, flooding was seen to occur in the tube above the junction—as in smaller diameter Ts, Azzopardi (1988). However, the phenomena observed in the series A experiments differed from those in the 0.032 m dia T in two ways. Firstly, there was a bend only 14 D beyond the T (c.f. 22 D in the 0.032 m case). There was obvious interaction with the bend with the possibility that liquid, which might have fallen down the main pipe, being taken into the horizontal main pipe after the bend and exiting via the run. Thus there would be less liquid than expected emerging through the side arm after falling back down to the junction. Secondly, the flooding waves did not appear to fill the entire pipe cross section as occurred in the smaller diameter tests. Therefore, liquid travelling in drop form would not all be captured and would not be taken off when flooding occurred. In the series B experiments the length of pipe between the junction and the bend was 30 D. Consequently there was not the same interaction with the bend as in the series A experiments.

At very low liquid flow rates an addition phenomenon was observed. Beyond a 'critical' amount of take off, the liquid travelling as a film appeared to come to a complete stop and built up as a collar around the main pipe at the junction. Most of this did not continue along the main pipe but was diverted into the side arm. Similar behaviour was reported by Azzopardi (1989) for a T junction with pipes of 0.032 m dia. An explanation for this phenomenon is given in section 2 above.

4.2. *Flow split data*

Phase flow split was measured in two series of experiments which differed in the geometry of the main pipe downstream of the junction. For each run the inlet flow rate were maintained constant, by using the valves on the outlet lines the full range of conditions between no take-off and total take-off could be explored. The nominal inlet conditions are given in table 2 whilst the flow split data are listed in the appendix. In the subsequent few figures, the flow split data are plotted as fraction of liquid taken off through the side-arm against fraction of gas.

Figure 3 shows data for runs A1 and B1, i.e. the same inlet conditions but different lengths of main pipe downstream of the junction. This illustrates the fact that there is more liquid taken off with the longer pipe, probably caused by the interaction between the flooding process and the bend hindering liquid falling back. Similar behaviour is seen in data from the other inlet flow rates. In the next four figures, series B data will be considered as no flooding/bend interaction was seen in these runs.

Table 2. Inlet conditions at which flow split was measured

Run No.	Inlet flow rates (kg/s)		Superficial velocities (m/s)		Length of downstream pipe (D)
	Gas	Liquid	Gas	Liquid	
A1	0.30	0.075	20.4	0.006	16
A2	0.31	0.250	21.0	0.02	16
A3	0.59	0.075	40.0	0.006	16
A4	0.58	0.254	39.4	0.02	16
B1	0.328	0.076	22.3	0.006	30
B2	0.328	0.252	22.3	0.02	30
B3	0.58	0.076	39.4	0.006	30
B4	0.59	0.252	40.0	0.02	30

In figures 4 and 5, it is seen that increasing the liquid flow rate at the inlet to the junction results in a decrease in the fraction of liquid taken off. This trend is similar to that observed in earlier experiments with a vertical main pipe but smaller diameter tubes, Azzopardi (1988). The trend also appears in data from junctions with horizontal main pipes, Shoham *et al.* (1987), Hart *et al.* (1991). The effect of inlet gas flow rate has also been studied, figure 6. This shows that the fraction of liquid taken off increases with increase in the gas velocity.

Data from junctions of two different diameters has been compared in figure 7. The experiments reported by Azzopardi (1988) were obtained from experiments with a junction made up of 0.032 m dia pipes and at a pressure of 1.5 bar. It has been shown by Azzopardi & Memory (1989) that data from different pressures give similar trends if their momentum for the phases, as $\rho_i u_i^2$, where i refers to gas or liquid, are the same. u_i is the superficial velocity for the phase i. The data in figure 7 are from available runs whose momentum gave the best match. Values of the momentum based on superficial velocities are given in table 3. Also listed are values of momentum based on local mean phase velocities.

The split of liquid between drops and wall film was calculated using the equation of Govan *et al.* (1988). For the film velocity, the equation for film thickness suggested by Willetts (1987) was employed. Drop velocities were assumed to be equal to the gas superficial velocity. This assumption is justified by the measurements of Azzopardi & Teixeira (1992).

It is of interest to note that the momentum values based on local values are about the same in both cases. From this point of view it is not surprising that the data from the two experiments are so similar. However, the difference in split between the drops and film does appear to contradict the idea that the split is governed by the reaction of film or drops to the movement of the gas as there is more liquid entrained in the larger diameter case.

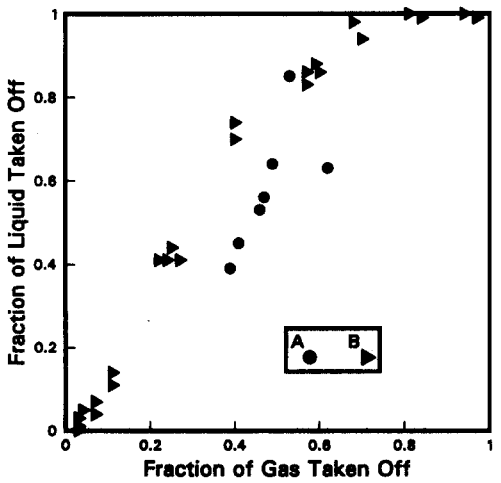

Figure 3. Effect of length of main pipe downstream of junction—superficial liquid velocity 0.02 m/s—superficial gas velocity 22 m/s—main pipe diameter side arm diameter 0.125 m—pressure 1 bar—series A 16 D, series B 30 D.

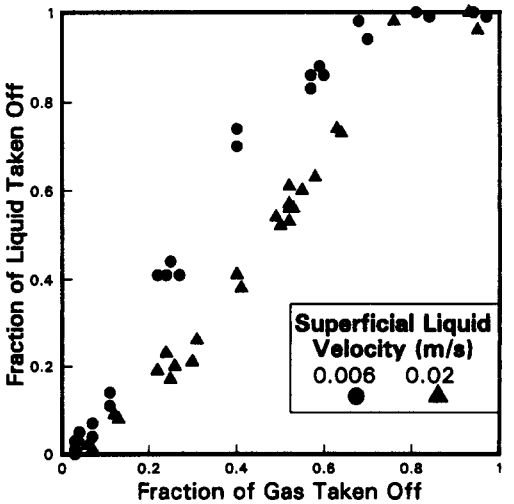

Figure 4. Effect of inlet liquid flow rate on flow split—superficial gas velocity 22 m/s—main pipe diameter = side arm diameter 0.125 m—pressure 1 bar.

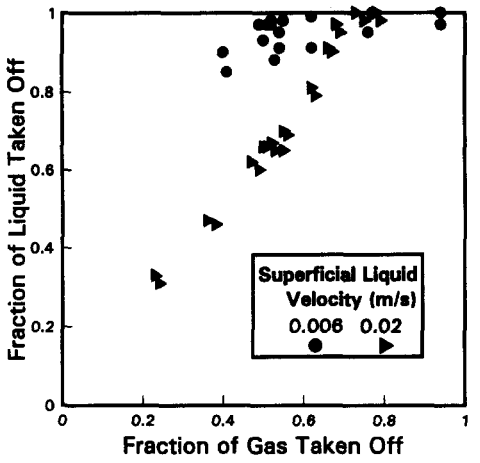

Figure 5. Effect of inlet liquid flow rate on flow split—superficial gas velocity 40 m/s—main pipe diameter = side arm diameter 0.125 m—pressure 1 bar.

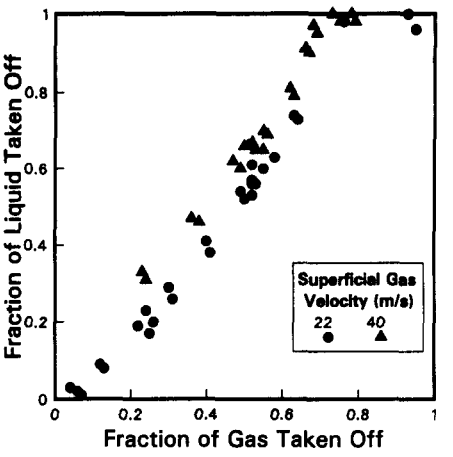

Figure 6. Effect of inlet gas flow rate on flow split—superficial liquid velocity 0.02 m/s—main pipe diameter = side arm diameter 0.125 m—pressure 1 bar.

4.3. Comparison with flow split models

The data obtained in the present work has been compared with predictions from available models, i.e. Shoham *et al.* (1987), Sliwicki & Mikielwicz (1988), Azzopardi (1989) and Hart *et al.* (1991). Though the models of Shoham *et al.* and Hart *et al.* were developed in conjunction with experiments on horizontal junctions, there is nothing in the physics underlying the models to prevent their being applied to vertical annular flow. Data from the series B experiments were chosen to test the published models as there was less interaction with the bend downstream of the junction. The experimental data are compared against predictions in figures 8 and 9. This shows that none of the models give consistently good predictions. For the models of Sliwicki & Mikieliwicz and Hart *et al.*, allowance was made for the fact that some liquid would be entrained. Not making this allowance would have led to lower liquid take-off being predicted. This could have resulted in poorer predictions. No allowance for entrainment was included in the Shoham *et al.* model. Including for this effect would have resulted in higher liquid take off being predicted and poorer agreement with data.

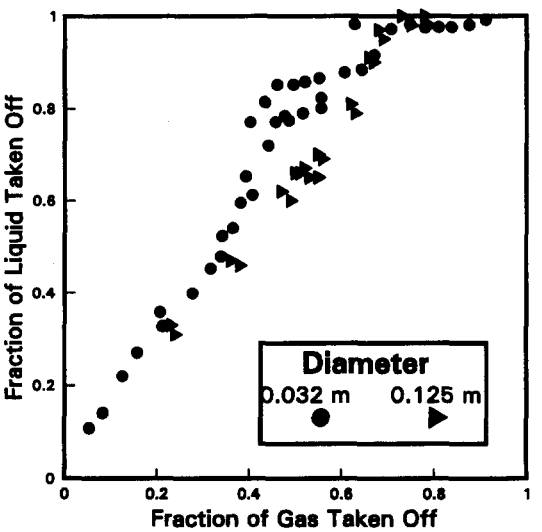

Figure 7. Effect of pipe diameter on flow split—present data, main pipe and side-arm diameter 0.125 m (superficial liquid velocity 0.02 m/s; superficial gas velocity 40 m/s; pressure 1 bar), and that of Azzopardi (1988), main pipe and side-arm diameter 0.032 m (superficial liquid velocity 0.016 m/s; superficial gas velocity 37.5 m/s; pressure 1.5 bar).

Table 3. Comparison of momentum from small and large diameter cases

Pipe diameter (m)	0.127	0.032
Gas momentum based on superficial velocity (kg/ms^2)	1926	2528
Liquid momentum based on superficial velocity (kg/ms^2)	0.043	0.25
Drop momentum (kg/ms^2)	1.6×10^6	1.4×10^6
Film momentum (kg/ms^2)	345	809
Entrained fraction	0.71	0.14

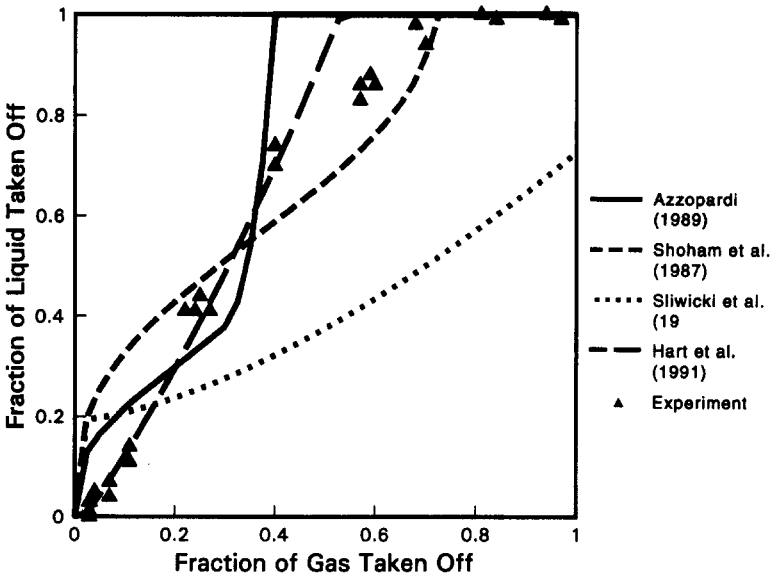

Figure 8. Comparison between experimental data and predictions of available models—superficial liquid velocity 0.006 m/s—superficial gas velocity 22 m/s—main pipe diameter = side arm diameter = 0.125 m—pressure = 1 bar.

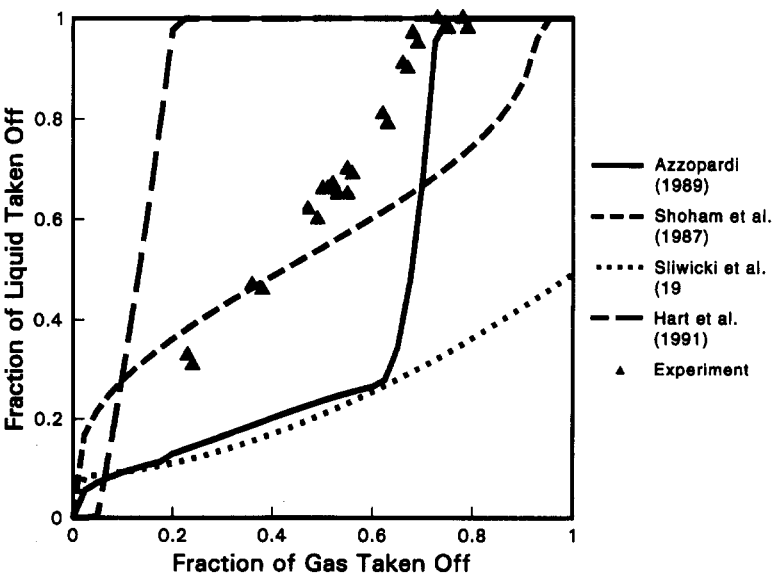

Figure 9. Comparison between experimental data and predictions of available models—superficial liquid velocity 0.02 m/s—superficial gas velocity 40 m/s—main pipe diameter = side arm diameter = 0.125 m—pressure = 1 bar.

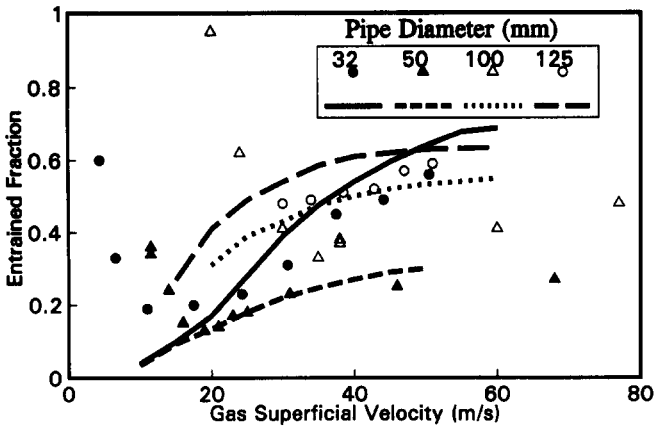

Figure 10. Variation of entrained fraction with gas velocity for different diameter tubes (0.032 m—Whalley & Azzopardi (1980) and Azzopardi & Baker (1981)—$u_l = 0.08$ m/s; 0.05 m—Verbeek *et al.* (1992)—$u_l = 0.013$ m/s; 0.1 m—Verbeek *et al.* (1992)—$u_l = 0.01$ m/s; 0.127 m—Azzopardi *et al.* (1983)—$u_l = 0.01$ m/s). Curves are predictions of Govan *et al.* (1988).

In the case of the model of Azzopardi (1989) the assumptions made have been reviewed to ensure that they were applicable to the conditions of the present experiments. Two items were identified for attention. Originally, it was assumed that the flooding process will cause all entrained drops to deposit onto the wall film and thence fall back and be taken off. Whilst this might be a reasonable assumption in small diameter junctions, it is probably not justified for the present larger scale where the flooding wave will not block as much of the main pipe cross-section. A more correct description might consider that drop deposition occurs more gradually and depends on the available length of downstream pipe. As a circulation zone is expected to occur in the main pipe just downstream of the T, this distance may not be the same as that between the T and the bend at the top of the vertical section.

The model of Azzopardi (1989) uses the division of liquid between drops and film (entrained fraction) in calculating the phase split. The entrained fraction is calculated from the correlation of Goven *et al.* (1988). For the higher gas flow rate runs, B3 and 4, figure 10 shows that the correlation gives reasonably good predictions. However, for the (lower) gas velocities corresponding to runs, B1 and 2, there is evidence that the Govan *et al.* correlation might be underpredicting

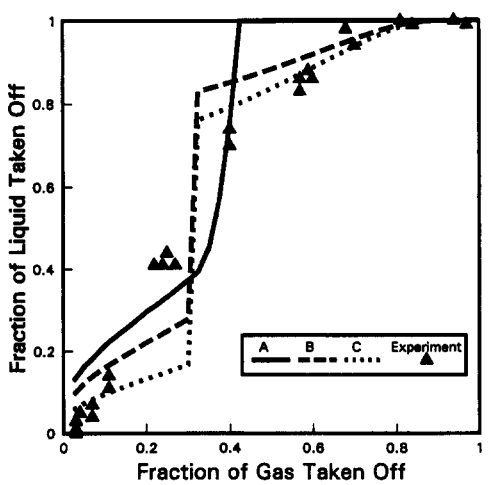

Figure 11. Comparison between experimental data and predictions of modified model of Azzopardi (1989)—superficial liquid velocity 0.006 m/s—superficial gas velocity 22 m/s—main pipe diameter = side arm diameter = 0.125 m—pressure = 1 bar. A—entrained fraction 0.33, all drops deposited; B—entrained fraction 0.5, deposition over 4 m; C—entrained fraction 0.7, deposition over 4 m.

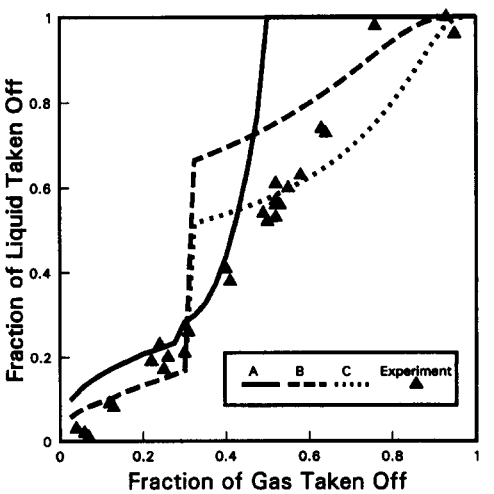

Figure 12. Comparison between experimental data and predictions of modified model of Azzopardi (1989)—superficial liquid velocity 0.02 m/s—superficial gas velocity 22 m/s—main pipe diameter = side arm diameter = 0.125 m—pressure = 1 bar. A—entrained fraction 0.49, all drops deposited; B—entrained fraction 0.7, deposition over 4 m; C—entrained fraction 0.7, deposition over 2 m.

significantly. At the higher gas flows, experiment data show the entrained fraction increasing monotonically with increasing gas velocity. In contrast, the experimental data illustrated in figure 10 indicates a contrary trend. The correlation only has an increasing trend.

Predictions made with a modification of the model of Azzopardi (1989) incorporating the above ideas are shown in figures 11 and 12. In the calculations presented here, empirical values are used for entrained fraction and deposition length as no, more theoretical, alternatives are available. In both cases, the original prediction is shown. For the lower liquid flow rate this results in an entrained fraction of 0.33. It can be seen in figure 11 that entrained fractions of 0.5 or 0.7 and gradual deposition over 4 m appear to give improved predictions. For the higher liquid flow rate increasing the entrained fraction from 0.49 (from Govan *et al.* 1988) to 0.7 and using gradual deposition over 2 or 4 m gives a similar improvement. As the actual distance between the T and the top band is 4 m the values used appear sensible. The entrained fractions selected are in keeping with the data trends illustrated in figure 10.

The possible problems of back up of liquid in the side-arm, identified above, indicate that further tests with are required with an alternative configuration in the side-arm.

5. CONCLUSIONS

From the above the following conclusions can be drawn:

(1) The phenomena which occur during the split of vertical annular flow at a vertical T junction of 0.125 m dia are very similar to those observed in earlier experiments in 0.032 m pipes.
(2) Interaction was observed between the flooding in the pipe above the junction and the bend beyond the junction when the distance between them is only 16 D.
(3) None of the published models gave consistently good predictions of the data. However, modifications to the model of Azzopardi (1989) which were based on observed phenomena gave improved agreement between predictions and experiment. These changes contain a great deal of empiricism and further work is required to set the ideas onto a sounder footing.

Acknowledgements—The experiments described in this paper were undertaken as part of the Underlying Research Programme of the UKAEA. The author would like to thank Dr K. T. Claxton (formerly of the Harwell Laboratory), Mr P. A. Smith (AEA Petroleum Services, Harwell) and Mr S. D. Taylor and Miss C. Rimmer (students from the University of Bradford attached to the Harwell Laboratory) for their assistance in carrying out the experiments.

REFERENCES

AZZOPARDI, B. J. & BAKER, S. R. 1981 Two phase flow in a T junction: the effect of flow pattern in vertical upflow. UKAEA Report AERE R10174.

AZZOPARDI, B. J. & WHALLEY, P. B. 1982 The effect of flow pattern on two phase flow in a T junction. *Int. J. Multiphase Flow* **8,** 481–507.

AZZOPARDI, B. J. 1984 The effect of side arm diameter on two phase flow split at a T junction. *Int. J. Multiphase Flow* **10,** 509–512.

AZZOPARDI, B. J. 1988 Measurements and observations of the split of annular flow at a vertical T junction. *Int. J. Multiphase Flow* **14,** 701–710.

AZZOPARDI, B. J. 1989 The split of annular-mist flows at vertical and horizontal Ts. *Proc. Eighth Int, Conf. on Offshore Mechanics and Artic Engineering*, The Hague, The Netherlands, 19–23 March, ASME.

AZZOPARDI, B. J. 1989 The split of annular-mist flows at vertical and horizontal Ts. *Proc. Eighth Int. Conf. on Offshore Mechanics and Arctic Engineering*, The Hague, The Netherlands, 19–23 March, ASME.

AZZOPARDI, B. J. & MEMORY, S. B. 1989 The split of two-phase flow at a horizontal T—annular and stratified flow. *4th Int. Conf. on Multiphase Flow*, Nice, France, 19–21 June (Pub. BHRA).

AZZOPARDI, B. J. & TEIXEIRA, J. C. F. 1982 Gas core turbulence and drop vehicles in vertical annular two-phase flow. *ASME Symp. on Basic Aspects of Two Phase Flow and Heat Transfer HTD*, Vol. 197, pp. 37–46, National Heat Transfer Conference, San Diego, Calif., 9–12 August.

BRAUNER, N. & BARNEA, D. 1986 Slug/churn transition in upward gas–liquid flow. *Chem. Engng Sci.* **41,** 159–163.

FOUDA, A. E. 1975 Two-phase flow behaviour in manifolds and networks. Ph.D. thesis, University of Waterloo, Canada.

GANDELL, A. 1957 Les pertes de charge dans les ecoulements au travers de branchements ente. *Bull. Technique Suisse Romande* **9,** 122–130 et **10,** 363–391.

GOVAN, A. H., HEWITT, G. F., OWEN, D. G. & BOTT, T. R. 1988 An improved CHF modelling code. *2nd U.K. National Heat Transfer Conf.*, Strathclyde University, Glasgow.

HART, J., HAMERSMA, P. J. & FORTUIN, J. M. H. 1991 Route selectivity for gas–liquid flow in horizontal T junctions. *Chem. Engng Sci.* **36,** 805–808.

HEWITT, G. F., GILL, L. E., ROBERTS, D. N. & AZZOPARDI, B. J. 1990 The split of low inlet quality gas/liquid flow at a vertical T—experimental data. UKAEA Report AERE M3801.

HONAN, T. J. & LAHEY, R. T. 1981 Measurement of phase separation in wyes and tees. *Nucl. Engng Des.* **64,** 93–102.

HWANG, S. T. 1986 A study on phase separation phenomena in branching conduits. Ph.D. thesis, Rensselear Polytechnic Institute, Troy, New York.

HWANG, S. T., SOLIMAN, H. M. & LAHEY, R. T. 1988 Phase separation in dividing two-phase flow. *Int. J. Multiphase Flow* **14,** 439–458.

MCQUILLAN, K. W. & WHALLEY, P. B. 1985 Flow patterns in vertical two-phase flow. *Int. J. Multiphase Flow* **11,** 161–175.

SHOHAM, O., BRILL, J. P. & TAITEL, Y. 1987 Two-phase flow splitting in a Tee junction—experiment and modelling. *Chem. Engng Sci.* **42,** 2667–2676.

SHOHAM, O., ARIRACHAKARAN, S. & BRILL, J. P. 1989 Two phase flow splitting in a horizontal reduced pipe tee. *Chem. Engng Sci.* **44,** 2388–2391.

SLIWICKI, E. & MIKIELIWICZ, J. 1988 Analysis of an annular-mist flow model in a T junction. *Int. J. Multiphase Flow* **14,** 321–331.

TAITEL, Y., BARNEA, D. & DUKELR, A. E. 1980 Modelling flow pattern transitions for steady upward gas-liquid flow in vertical tubes. *AIChEJl* **26,** 345–354.

VERBEEK, P. H. J., MIESEN, R. & SCHELLEKENS, C. J. 1992 Liquid entrainment in annular dispersed upflow. *8th Annual European Conf. on Liquid Atomisation and Spray Systems*, Amsterdam, 30 September–2 October.

WALLIS, G. B. 1961 Flooding velocities for air and water in a vertical tube. UKAEA Report AEEW R123.

WILLETTS, I. P. 1987 Non-aqueous annular two-phase flow. D.Phil. thesis, University of Oxford.

ZETZMANN, K. 1982 Phasen separation und druckabfall in zweiphasig durchstroemten vertikalen rohrabzweigen. Dr.Ing. thesis, University of Hanover, Germany.

APPENDIX A

Flow Split Data

Run No.	Flow rate (kg/s)				Fractional take-off	
	Side-arm		Run			
	Gas	Liquid	Gas	Liquid	Gas	Liquid
A1	0.134	0.033	0.197		0.41	0.45
	0.146	0.040	0.170		0.46	0.53
	0.205	0.40	0.138		0.62	0.63
	0.179	0.063	0.158		0.53	0.85
	0.163	0.041†	0.170	0.026	0.49	0.64
	0.154	0.038†	0.173	0.033	0.47	0.56
	0.124	0.023†	0.193	0.045	0.39	0.39

continued overleaf

Appendix A continued

Run No.	Flow rate (kg/s)				Fractional take-off	
	Side-arm		Run			
	Gas	Liquid	Gas	Liquid	Gas	Liquid
A2	0.122	0.055	0.186		0.40	0.20
	0.143	0.078	0.173		0.45	0.31
	0.186	0.083	0.128		0.59	0.33
	0.161	0.073	0.153		0.51	0.29
	0.147	0.053†	0.155	0.183	0.49	0.26
	0.136	0.046†	0.166	0.183	0.45	0.26
	0.143	0.060†	0.159	0.186	0.47	0.25
	0.157	0.060†	0.147	0.181	0.52	0.27
A3	0.262	0.058	0.326		0.45	0.77
	0.299	0.068	0.293		0.51	0.92
	0.356	0.063	0.224		0.62	0.84
	0.332	0.057	0.263		0.57	0.77
	0.337	0.069†	0.275	0.004	0.55	0.95
	0.245	0.062†	0.334	0.009	0.42	0.83
A4	0.229	0.117	0.351		0.39	0.46
	0.285	0.125	0.303		0.48	0.49
	0.370	0.158	0.230		0.62	0.63
	0.338	0.141	0.260		0.57	0.56
B1	0.322	0.075			0.97	0.99
	0.010	0.0			0.03	0.0
	0.080	0.031			0.24	0.41
	0.136	0.052			0.40	0.70
	0.010	0.001			0.03	0.01
	0.036	0.008			0.11	0.11
	0.024	0.003			0.07	0.04
	0.088	0.031			0.27	0.41
	0.279	0.075			0.84	0.99
	0.232	0.071			0.70	0.94
	0.201	0.065			0.60	0.86
	0.190	0.063			0.57	0.83
			0.310	0.0	0.94	1.00
			0.010	0.073	0.03	0.03
			0.073	0.045	0.22	0.41
			0.134	0.020	0.40	0.74
			0.012	0.071	0.04	0.05
			0.035	0.065	0.11	0.14
			0.023	0.070	0.07	0.07
			0.083	0.042	0.25	0.44
			0.068	0.0	0.81	1.00
			0.225	0.001	0.68	0.98
			0.196	0.009	0.59	0.88
			0.188	0.010	0.57	0.86
B2	0.176	0.139			0.53	0.56
	0.175	0.139			0.53	0.56
	0.183	0.149			0.55	0.60
	0.211	0.182			0.64	0.73
	0.248	0.243			0.76	0.98
	0.314	0.239			0.95	0.96
	0.172	0.134			0.52	0.53
	0.163	0.131			0.50	0.52
	0.134	0.095			0.41	0.38
	0.085	0.050			0.26	0.20
	0.023	0.003			0.07	0.01
	0.087	0.044			0.25	0.17
	0.103	0.066			0.31	0.26
	0.044	0.019			0.13	0.08
			0.174	0.096	0.52	0.61
			0.171	0.106	0.52	0.57
			0.181	0.092	0.58	0.63
			0.205	0.065	0.63	0.74
			0.243	0.001	0.93	1.00
			0.304	0.0	0.93	0.56
			0.169	0.111	0.52	0.54
			0.161	0.117	0.49	0.41
			0.132	0.150	0.40	0.23

continued opposite

Appendix A continued

Run No.	Flow rate (kg/s)				Fractional take-off	
	Side-arm		Run			
	Gas	Liquid	Gas	Liquid	Gas	Liquid
B2			0.080	0.194	0.24	0.03
			0.012	0.245	0.04	0.02
			0.020	0.246	0.06	0.19
			0.071	0.204	0.22	0.21
			0.100	0.179	0.30	0.21
			0.040	0.229	0.12	0.09
B3	0.302	0.066			0.52	0.88
	0.306	0.069			0.53	0.91
	0.313	0.068			0.54	0.91
	0.361	0.071			0.62	0.95
	0.439	0.072			0.76	0.97
	0.516	0.081			0.94	0.95
	0.313	0.070			0.54	0.93
	0.292	0.071			0.50	0.93
	0.238	0.064			0.41	0.85
			0.294	0.002	0.51	0.97
			0.302	0.002	0.52	0.98
			0.317	0.002	0.55	0.98
			0.357	0.001	0.62	0.99
			0.443	0.0	0.77	1.00
			0.515	0.0	0.94	1.00
			0.298	0.002	0.52	0.97
			0.283	0.002	0.49	0.97
			0.007	0.007	0.40	0.90
B4	0.321	0.164			0.55	0.65
	0.319	0.165			0.55	0.65
	0.328	0.173			0.56	0.69
	0.369	0.199			0.63	0.79
	0.432	0.246			0.75	0.98
	0.310	0.164			0.53	0.65
	0.288	0.152			0.49	0.60
	0.220	0.117			0.38	0.46
	0.134	0.079			0.24	0.31
	0.458	0.248			0.79	0.98
	0.404	0.240			0.69	0.95
	0.390	0.223			0.67	0.90
			0.298	0.086	0.51	0.66
			0.302	0.083	0.52	0.67
			0.321	0.076	0.55	0.70
			0.359	0.047	0.62	0.81
			0.421	0.001	0.73	1.00
			0.289	0.085	0.50	0.66
			0.275	0.096	0.47	0.62
			0.211	0.133	0.36	0.47
			0.131	0.170	0.23	0.33
			0.451	0.0	0.78	1.00
			0.396	0.008	0.68	0.97
			0.380	0.024	0.66	0.91

†Deduced by difference.